Energy 172 (2019) 592–598

Contents lists available at ScienceDirect

Energy

journal homepage: www.elsevier.com/locate/energy

Pressure retarded osmosis: Operating in a compromise between power density and energy efficiency

Rui Long*, Xiaotian Lai, Zhichun Liu, Wei Liu**

School of Energy and Power Engineering, Huazhong University of Science and Technology, 1037 Luoyu Road, Wuhan, 430074, China

ARTICLE INFO

Article history:
Received 2 March 2018
Received in revised form
29 January 2019
Accepted 31 January 2019
Available online 1 February 2019

Keywords:
Pressure retarded osmosis (PRO)
Single objective optimization
Multi-objective optimization
Power density
Energy efficiency

ABSTRACT

Pressure retarded osmosis (PRO) is a promising technology for salinity gradient energy utilization. Here, based on previous literature, we proposed a simplified model to describe the PRO process, which was validated by a great accordance with the experimental data of water flux and power density. A sensitivity analysis of the PRO system indicated that there exist different optimal hydraulic pressure differences leading to the maximum power density and energy efficiency, respectively. The performance of the PRO system under the maximum power density and energy efficiency is systematically investigated based on the GA method. Furthermore, the Pareto front that indicates any arbitrary compromise between the maximum power density and energy efficiency based on NSGA-II was obtained. Factors determining the choice of the final compromise solution in the Pareto frontier remains are systematically discussed, which should be referred to the local energy policies and technical and economic conditions of the PRO systems. For demonstration, the final compromise solution selected by the abstract heuristic TOPSIS method is discussed and a desirable compromise between the power density and energy efficiency is presented.

1. Introduction

Due to fast depletion of traditional fuel energy and increasing energy demand induced by population expansion, environment suffers much, such as global warming and air pollution [1]. Exploiting new and renewable energy, developing high efficient energy conversion devices for traditional energy, and reutilizing waste thermal energy pave ways to alleviate such diploma [2,3]. Among them, salinity gradient technologies that could use the vastly existing Gibbs free energy of mixing of sea water, that can potentially generate electricity for 13% of global electricity consumption [4], provide a promising alternative for electricity generation, such as pressure retarded osmosis (PRO), reverse electrodialysis (RED) and capacitive mixing (CAPMIX) [5–12]. Compared with the other two technologies, PRO presents the advantage of satisfied power density and energy efficiency, which is being extensively investigated [13–17].

In the PRO process, water from the diluted feed solution permeates through a semipermeable membrane into a pressurized, concentrated draw solution, and then is depressurized through a hydro turbine to generate electricity. As a membrane based technology, the performance of the PRO system is significantly impacted by the semipermeable membrane characteristics, structure configuration, as well as operating conditions. She et al. [18] systematically investigated the effects of concentration and temperature of the feed and draw solutions, membrane type and orientation, and reverse solute diffusion on the performance of a PRO system. In the PRO process, both external concentration polarization (ECP) and internal concentration polarization (ICP) occur. The ECP leads to decreased concentration at the membrane-solution interface in the draw solution, and the ICP results in that the concentration at the membrane-solution interface deviates from that of the bulk feed solution. Furthermore, as the nature of the imperfect membrane, which could not completely prevent the salt diffusion across the membrane, a reverse salt permeation (RSP) exists. The existence of the ECP, ICP, and RSP could degrade the performance of the PRO systems [19–21]. He et al. [22] proposed a simplified PRO model which considers the impacts of ECP, ICP, and RSP, and revealed that the extractable energy could be significantly reduced due to the ICP, ECP and RSP effects.

Much efforts have been focused on the power density of the PRO system. Yip et al. [23] developed a theoretical model to predict the

* Corresponding author.
** Corresponding author.
E-mail addresses: r_long@hust.edu.cn (R. Long), w_liu@hust.edu.cn (W. Liu).

https://doi.org/10.1016/j.energy.2019.01.169
0360-5442/

water flux and power density. Kim et al. [24] designed a new PRO crossflow system featured with asymmetric channels to prevent membrane stretching and bulging. Yaroshchuk [25] investigated the optimal hydrostatic counter-pressure. Kim et al. [26] analyzed the influence of feed channel spacers on the performance of PRO system. Kim et al. [27] pointed out that there is a critical need to optimize feed channel spacers to minimize membrane deformation and the "shadow effect", thus to achieve high power densities. Furthermore, Nagy et al. [28] found that essential improvement of the membrane selectivity and/or decrease of the value of the structural parameter is beneficial for energy extraction. Two stage PRO systems are also constructed to improve the power density. He et al. [29] presented a two-stage PRO process to enhance the energy extraction. To avoid the feed water pretreatment, closed-loop PRO systems are also developed. Han et al. [30] conceived a novel closed-loop PRO process, which exhibits advantages of sustainable high power output, negligible internal concentration polarization and low membrane fouling. Anastasio et al. [31] investigated the impact of temperature on power density in closed-loop PRO for grid storage. Long et al. [32]developed an energy storage system based on the PRO and the RO systems.

For improving the performance of the PRO system, previous literature are mainly dedicated to the maximum power density. Few literature have considered its energy efficiency. Energy efficiency reflects the utilization degree of the Gibbs free energy of mixing of the draw and feed solutions, and acts as an evaluation of the system conversion ability. In addition, in the area with abundant brine water and shortage of river water, the energy efficiency and power density should both be included for economical utilization and water saving. In this paper, we developed a simplified model which includes the ICP, ECP, and RSP to investigate the performance of the PRO system under different hydraulic pressure differences. To achieve the optimal operation conditions, performance optimizations under the single objective optimization for power density and energy efficiency were, respectively, conducted. Furthermore, as the power density and energy efficiency could not achieve their maximum values simultaneously, to coordinate this contradiction, we conducted a multi-objective optimization to obtain the Pareto frontier that indicates any arbitrary compromise between the maximum power density and energy efficiency. Factors determining the choice of the final compromise solution in the Pareto frontier remains are systematically discussed. For demonstration, the final compromise solution selected by the abstract heuristic TOPSIS method is presented.

2. Model development

In the PRO process, water (J_w) transfers from the diluted feed solution to the concentrated draw solution due to the osmotic effect and salt flux (J_s) diffuse through the membrane from the draw solution to the feed one. Here we denote V and C as the volume flow rate and concentration, respectively. D and F refer to draw and feed solutions. As shown in Fig. 1, at position x, for an infinitesimal length Δx, in the flow direction, according to the mass balance, we have

$$V_D(x+\Delta x) = V_D(x) + J_w(x)W\Delta x \tag{1}$$

$$V_F(x+\Delta x) = V_F(x) - J_w(x)W\Delta x \tag{2}$$

where W is membrane width. Compared to the channel height, the thickness of the dense layer is relatively small, therefore, the bulk concentration can be treated as the average concentration along the flow direction. Hence, the bulk concentrations of the draw and feed solutions at $x+\Delta x$ can be deduced as

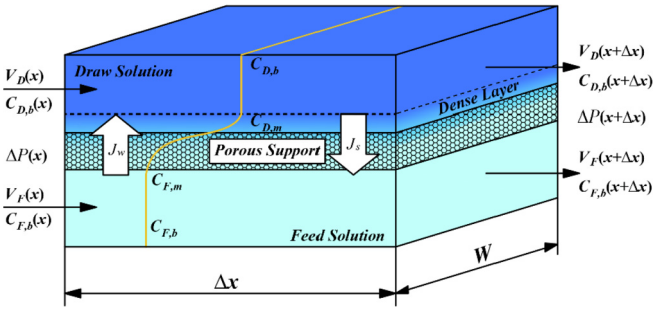

Fig. 1. Mass transfer characteristics along the flow direction in an infinitesimal length.

$$C_{D,b}(x+\Delta x) = \frac{V_D(x)C_{D,b}(x) - J_s(x)W\Delta x}{V_D(x+\Delta x)} \tag{3}$$

$$C_{F,b}(x+\Delta x) = \frac{V_F(x)C_{F,b}(x) + J_s(x)W\Delta x}{V_F(x+\Delta x)} \tag{4}$$

According to Eqs. (1)–(4), the differential equations governing the volume flow rate and concentration variations along the flow direction can be, respectively, expressed as

$$dV_D(x) = J_w(x)Wdx \tag{5}$$

$$dV_F(x) = -J_w(x)Wdx \tag{6}$$

$$\frac{dC_{D,b}(x)}{dx} = \frac{-J_s(x)W - C_{D,b}(x)J_w(x)W}{V_D(x)} \tag{7}$$

$$\frac{dC_{F,b}(x)}{dx} = \frac{J_s(x)W + C_{F,b}(x)J_w(x)W}{V_F(x)} \tag{8}$$

The local water flux at position x can be evaluated by Ref. [33].

$$J_w(x) = A(\Delta\pi_m(x) - \Delta P(x)) \tag{9}$$

where A is the water permeability coefficient, $\Delta\pi_m$ is the local osmotic pressure difference aside the membrane, ΔP is the local hydraulic pressure difference across the membrane.

Usually, the hydrophilic membrane can not prevent all the ions from piercing through the membrane as we want. Due to the diffusion effect, there exist a salt flux from the concentrated draw solution to the diluted feed solution [34,35].

$$J_s(x) = B(C_{D,m}(x) - C_{F,m}(x)) \tag{10}$$

where B is the salt permeability coefficient, which can be determined through RO experiments. $C_{D,m}$ and $C_{F,m}$ are the concentrations of the draw solution and feed solution at the membrane side.

Induced by the ICP, the relation of the concentrations at the membrane-solution interface and the bulk solution for the feed solution is [23].

$$C_{F,m} = C_{F,b}\exp(KJ_w) + \frac{B}{J_w}(C_{D,m} - C_{F,m})(\exp(KJ_w) - 1) \tag{11}$$

where $K = \frac{S}{D}$ is the solute resistivity. S is the structural parameter [36]. D is the diffusion coefficient of the draw solution. The impact of ICP is illustrated by the first term on the right-hand side, where the bulk feed solution concentration is magnified by $\exp(KJ_w)$. The second term allows for the increase in salt concentration at the

membrane interface due to the RSP.

Due to the ECP resulted by transmembrane water through the membrane, which dilutes the draw solution at the dense layer, the relation of the concentrations at the membrane-solution interface and the bulk solution for the draw solution is [23].

$$C_{D,m} = C_{D,b}\exp\left(-\frac{J_w}{k}\right) - \frac{B}{J_w}(C_{D,m} - C_{F,m})\left(1 - \exp\left(\frac{J_w}{k}\right)\right) \tag{12}$$

where k is the local mass transfer coefficient [37]. We can see that $C_{D,m}$ depends on two terms. The first term describes the bulk draw concentration, $C_{D,b}$, corrected by $\exp\left(-\frac{J_w}{k}\right)$, and the second term indicates the concentration decrease due to RSP.

To meet actual conditions, pressure drops along the flow direction in the feed and draw solution channels are calculated. Due to the turbulent nature of flow for spacer filled channels, the local solution pressure loss (P_{loss}) at position x are [34].

$$P_{loss} = \frac{\lambda\rho v^2 x}{2d_h} \tag{13}$$

where ρ and v are the density and cross flow velocity, respectively. d_h is the hydraulic diameter [38], and $\lambda = 6.23\mathrm{Re}^{-0.3}$ is the friction coefficient [34]. Hence, the local net hydraulic pressure difference (ΔP) across the membrane is given as [34]:

$$\Delta P(x) = \Delta P^0 - P_{loss,D}(x) + P_{loss,F}(x) \tag{14}$$

where ΔP^0 is the pressure difference of the draw and feed solutions at the inlet. The pressure difference at the outlet (L) is

$$\Delta P_{net} = \Delta P^0 - P_{loss,D}(L) + P_{loss,F}(L) \tag{15}$$

Therefore, the local water flux and salt flux can be expressed as [23,34].

$$J_w(x) = A\left(\frac{\pi_{D,b}(x)\exp\left(-\frac{J_w(x)}{k}\right) - \pi_{F,b}(x)\exp(KJ_w(x))}{1 + \frac{B}{J_w(x)}\left[\exp(KJ_w(x)) - \exp\left(-\frac{J_w(x)}{k}\right)\right]} - \Delta P(x)\right) \tag{16}$$

$$J_s(x) = B\left(\frac{C_{D,b}(x)\exp\left(-\frac{J_w(x)}{k}\right) - C_{F,b}(x)\exp(KJ_w(x))}{1 + \frac{B}{J_w(x)}\left[\exp(KJ_w(x)) - \exp\left(-\frac{J_w(x)}{k}\right)\right]}\right) \tag{17}$$

The distributions of the volume flow rate and concentration along the flow direction can be calculated by solving the governing mass transfer Eqs. (5)–(8) with the boundary conditions:

$$V_D(0) = V_D{}^0,\ V_F(0) = V_F{}^0,\ C_D(0) = C_D{}^0,\ C_F(0) = C_F{}^0,\ \Delta P(0) = \Delta P^0 \tag{18}$$

The transmembrane water $\Delta V_{PRO} = V_D(L) - V_D(0)$ equals to the difference of the inlet and outlet volume flow rates of the draw solution. The power output is $P_{PRO} = \Delta V_{PRO}\Delta P_{net}$. Therefore, the average water flux ($\bar{J}_w$) and power density (P_d) are

$$\bar{J}_w = \frac{\Delta V_{PRO}}{WL} = \frac{V_D(L) - V_D(0)}{WL} \tag{19}$$

$$P_d = \frac{P_{PRO}}{WL} = \frac{\Delta V_{PRO}\Delta P_{net}}{WL} = \bar{J}_w\Delta P_{net} \tag{20}$$

Energy efficiency, η, indicating the ratio between the electricity generated and the decrease of the Gibbs free energy of mixing is also employed to evaluate the performance:

$$\eta = \frac{P_{PRO}}{\Delta G_{mix,in} - \Delta G_{mix,out}} \tag{21}$$

where Gibbs free energy of mixing (ΔG_{mix}) can be expressed as [39].

$$\Delta G_{mix} = 2RT\left[V_H C_H \ln\frac{C_H}{C_T} + V_L C_L \ln\frac{C_L}{C_T}\right] \tag{22}$$

where C_T is the concentration of the mixed concentrated and diluted solutions.

3. Impacts of hydraulic pressure difference on the PRO performance

3.1. Model validation

The model presented in this paper is validated by the measured values of a small flat-sheet PRO system [37]. The channel is $L = 75$ mm length, $W = 25$ mm width, and $H = 2.5$ mm depth; The effective membrane area is 18.75 cm^2. The draw solution is 35 g/L NaCl aqueous solution and the feed solution is deionized (DI) water. The volume flow rates and temperatures for the draw solution and feed solution are identical, which are 0.5 L/min and 25 °C, respectively. The model studied in this paper can be justified by great agreement between the calculated transmembrane water flux as well as power density and experimental measured ones, as illustrated in Fig. 2.

3.2. Sensitivity analysis

According to aforementioned equations, for given configuration of PRO system, the hydraulic pressure difference between the draw and feed solutions and the concentrations of the draw and feed solutions play determinative roles on the PRO power density and energy efficiency. Here a small flat-sheet PRO system is employed.

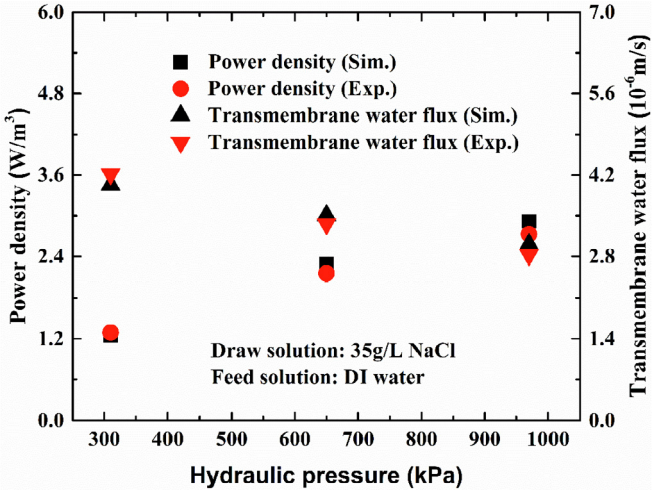

Fig. 2. Validation of the present model. Calculated and measured power densities and transmembrane water flux of a small flat-sheet PRO system as a function of the hydraulic pressure difference. The channel is $L = 75$ mm long, $W = 25$ mm wide, and $H = 2.5$ mm deep [37]; The effective membrane area is 18.75 cm^2. The draw solution is 35 g/L NaCl aqueous solution and the feed solution is deionized (DI) water. The volume flow rates for the draw solution and feed solution are identical, 0.5 L/min. The operation temperature is 25 °C.

The channel is $L = 75$ mm long, $W = 25$ mm wide, and $H = 2.5$ mm deep. The structural parameter is $S = 6.78 \times 10^{-4} m$. The water and salt permeability coefficients are, respectively, $A = 1.87 \times 10^{-12} m/(s \cdot Pa)$ and $B = 1.11 \times 10^{-7} (m/s)$. The impacts of the hydraulic pressure difference on the PRO performance under different draw and feed solution concentrations are systematically investigated.

Figs. 3 and 4 show the impacts of hydraulic pressure difference on the power density and energy efficiency of the PRO system under different feed and draw solution concentrations. The power density and energy efficiency both first increase with increasing hydraulic pressure difference, reach their maximum values, respectively, and then decrease. The optimal hydraulic pressure difference is slightly larger than half of the half osmotic pressure, which shows the same phenomenon with Ref. [25]. For given concentrations of the draw and feed solutions, with increasing hydraulic pressure difference, the driven force for the PRO system decreases, so does the utilized Gibbs free energy of mixing. The energy efficiency is defined as the ration of power output and the utilized Gibbs free energy of mixing. As the power has a maximum value, the energy efficiency also presents a maximum one, and the optimal hydraulic pressure difference corresponding to the maximum energy efficiency is larger than that corresponding to the maximum power density, as shown in Figs. 3 and 4. Furthermore, the maximum power density decreases with increasing feed solution concentration and decreasing draw solution concentration, as shown in Fig. 4, based on the fact that the increase of the feed solution concentration induces a decrease of the osmotic pressure difference aside the membrane, therefore the driven force of the PRO process decreases. Whereas, the maximum energy efficiency increases with increasing feed and draw solution concentrations, as depicted in Figs. 3 and 4.

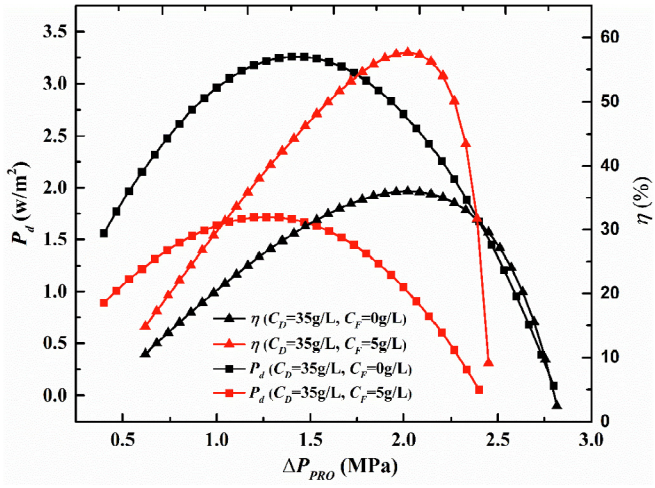

Fig. 3. Power density and energy efficiency as a function with hydraulic pressure difference under different feed solution concentrations.

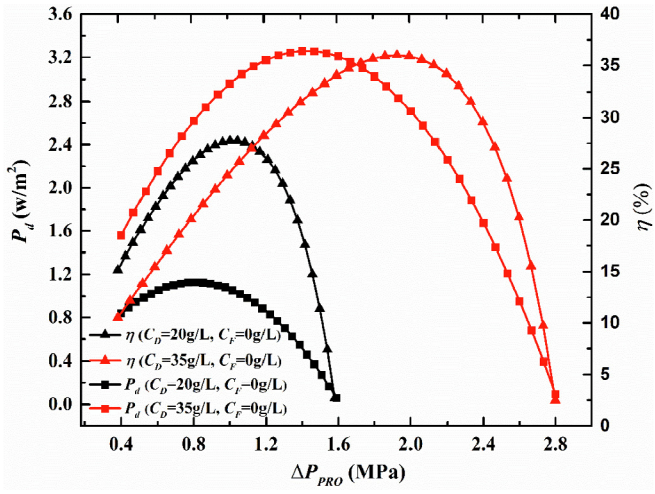

Fig. 4. Power density and energy efficiency as a function with hydraulic pressure difference under different draw solution concentrations.

4. Performance optimization

4.1. Performance under the maximum power density

Power density, indicating how much benefit we can get from the system, has been extensively researched for the PRO system. As mentioned in the sensitivity analysis, there exists an optimal hydraulic pressure difference leading to the power density of the PRO system. Conditioned on the system non-linearity, genetic algorithm (GA) method provides an alternative to calculate the optimal values of non-linear problems, which has been extensively applied in system optimizations [40,41]. In this section, we conducted a systematic investigation into the PRO performance based on GA method with the maximum power density as the optimization objective.

Fig. 5 shows the optimal hydraulic pressure difference, water flux, power density and energy efficiency as a function with feed solution concentration under the optimization for power density at different NaCl concentrations of the draw solution. The optimal hydraulic pressure difference, water flux and maximum power under maximum optimization for power density all decrease with increasing feed solution concentration. However, the energy efficiency under optimal condition increases with increasing feed solution concentration, as shown in Fig. 5(d), first dramatically, then much slowly at large values of the feed solution concentration. Furthermore, as depicted in Fig. 5, larger concentration of the draw solution leads to larger hydraulic pressure difference, larger water flux, hence larger power density and energy efficiency. Based on Eq. (20), larger concentration of the draw solution, larger hydraulic pressure difference, thus larger power density.

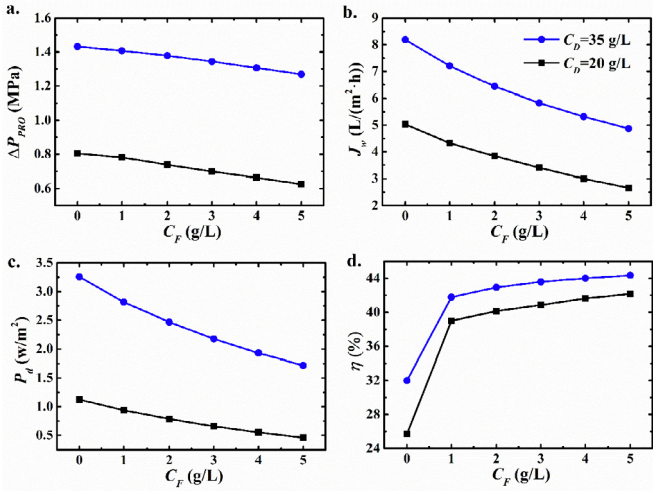

Fig. 5. Optimal hydraulic pressure difference, water flux, power density and energy efficiency as a function with feed solution concentration under the optimization for power density.

4.2. Performance under the maximum energy efficiency

Few literates have been focused on the energy efficiency of the PRO based on the fact that the draw and feed solution for the PRO system usually comes from the sea and river water, and are sufficient in a sense. However, for closed loop systems or in the area with shortage of river water, the energy efficiency, evaluating the utilization degree of the Gibbs free energy of mixing from the draw and feed solutions, should be also addressed for efficient conversion. According to the sensitivity analysis, there exists an optimal hydraulic pressure difference leading to the energy efficiency of the PRO system. Similarly, a systematic investigation into the PRO performance under the maximum energy efficiency is conducted.

Fig. 6 shows the optimal hydraulic pressure difference, water flux, power density and energy efficiency as a function with feed solution concentration under the optimization for energy efficiency at different NaCl concentrations of the draw solution. In Fig. 6(a), the optimal hydraulic pressure difference under maximum optimization for energy efficiency increases first with increasing feed solution concentration, reaches the maximum values, and then decrease. And larger concentration of the draw solution leads to larger hydraulic pressure difference. As shown in Fig. 6 (b), the water flux under the optimal conditions decreases monotonously with increasing feed solution concentration. And larger concentration of the draw solution leads to larger water flux due to larger driven force of the PRO process. As illustrated in Fig. 6 (c), the maximum power density decreases momentously with increasing feed solution concentration. And larger concentration of the draw solution leads to a larger value of the maximum power density because of the fact that larger draw solution concentration leads to larger hydraulic pressure difference and water flux, thus larger power density, based on Eq. (20). The optimal energy efficiency under optimal condition increases with increasing feed solution concentration, as shown in Fig. 6(d), first dramatically, then much slowly at large values of the feed solution concentration. And larger concentration of the draw solution leads to a larger value of the energy efficiency under the optimal condition.

4.3. Performance under the compromise condition

Multi-objective optimization can coordinate conflicting objectives, such as NSGA-II that has been extensively employed to achieve the compromise of the power and efficiency for energy conversion systems [42–44]. The results obtained by the multi-objective optimization are called Pareto frontier, which are a set of non-dominated solutions with minimum conflict between the objectives. Each solution in the Pareto frontier represents different weights of the conflicting objectives. As mentioned in the sensitivity analysis, the power density and energy efficiency of the PRO system cannot achieve their maximum values simultaneously. For economic operation and water saving, both the power density and energy efficiency should be addressed. And an optimization based on NSGA-II has been conducted to achieve an appropriate compromise between the energy efficiency and the power density.

4.3.1. Pareto frontier

Fig. 7 demonstrates the Pareto frontiers obtained via the multi-objective optimization under different feed solution concentrations with 35 g/L NaCl of draw solution, where obvious repugnant phenomenon of the maximum power density and maximum energy efficiency can be observed. Each solution in the Pareto frontier illustrates some certain weights of the power density and energy efficiency. For example, the far left or right solution means the energy efficiency or power density is mostly weighted, which is in accordance with the single objective optimization for energy efficiency or power density, respectively. Higher feed concentration leads to lower values of maximum power density, however, larger energy efficiency.

4.3.2. Final compromise solution in the pareto frontier

As each solution in the Pareto frontier represents different weights of the conflicting objectives, how to appropriately choose the final compromise solution in the Pareto frontier remains a dilemma. The cost and availability of water and the capital cost of changing the power in the system can significantly impact the choice of the final compromise solution. To decrease the PRO operating cost, the feasibility of water should be considered. In the areas lack of water, the cost of water could play a significant role in determining the overall operating benefit of the PRO system. In addition, the adaptable power output requires the redundant design of the power system, which significantly increasing the capital cost of building and operating PRO systems. Moreover, the

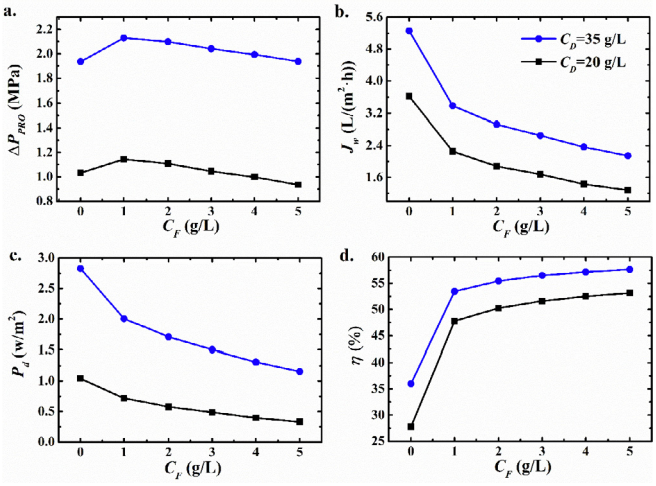

Fig. 6. Optimal hydraulic pressure difference, water flux, power density and energy efficiency as a function with feed solution concentration under different optimization objectives.

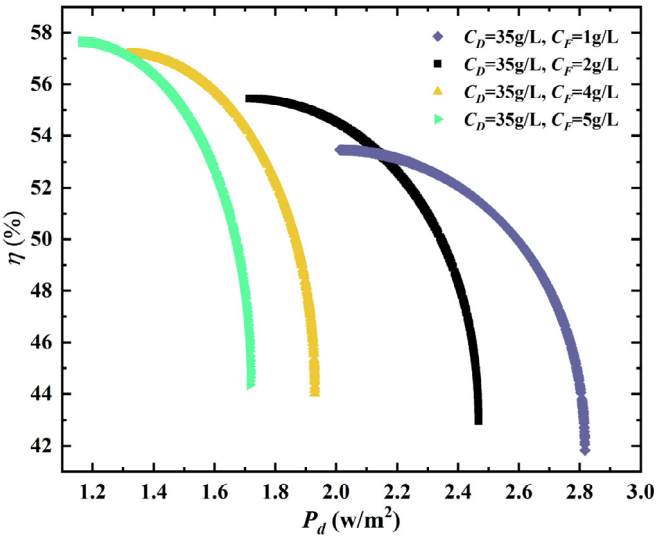

Fig. 7. Pareto frontier from multi-objective optimization of the PRO system under different feed solution concentrations. In the calculation, the draw solution concentration is 35 g/L.

Table 1
Performance comparisons under different optimization methods ($C_D = 35$ g/L).

feed solution concentration C_F (g/L)	multi-objective optimization compared to single-objective optimization (maximum P_d)		multi-objective optimization compared to single-objective optimization (maximum η)	
	P_d	η	P_d	η
0	−2.97%	+8.57%	+11.83%	−3.51%
1	−5.72%	+17.22%	+32.47%	−8.39%
2	−5.87%	+17.63%	+35.99%	−8.90%
3	−5.88%	+17.68%	+36.40%	−9.19%
4	−6.01%	+17.88%	+38.60%	−9.26%
5	−6.02%	+17.76%	+39.90%	−9.40%

local energy police can also affect the final compromised operating conditions, such as the feed-in tariff on the electricity price, as the operation of the PRO power system relies on salt and river water, which does not discharge pollutants and greenhouse gas to the environment. The final compromise solution should be determined by the local energy policies and technical and economic conditions of the PRO systems.

For demonstration, we have adopted the abstract heuristic TOPSIS method to select the final compromise solution in the Pareto frontier. TOPSIS represents the maximum deviation from the non-ideal solution and a minimum deviation from the ideal solution, indicating an abstract heuristic compromise. As shown in Table 1, when the NaCl concentration of the draw and feed solution are 35 g/L and 2 g/L, the power density under the multi-objective optimization is 5.87% less than the maximum one, but is 17.63% higher than that under the single objective optimization for energy efficiency. The energy efficiency under the optimization is 8.90% less than the maximum one, but is 35.99% higher than that under the single objective optimization for power density. When the feed solution is DI water, the energy efficiency under the optimization is slightly less than the maximum one, but is much higher than that under the single objective optimization for power density. The energy efficiency under the optimization is 3.51% less than the maximum one. However it is 11.83% higher than that under the single objective optimization for power density, meanwhile the power density under the multi-objective optimization is 2.97% less than the maximum one, but is 8.57% higher than that under the single objective optimization for energy efficiency.

5. Conclusions

In this paper, we developed a simplified mathematical model based on previous literature to investigate the impacts of operation parameters on the performance of the PRO system. This model considered the internal polarization concentration, external polarization concentration and reverse salt permeation, which was validated by a great accordance with the experimental data of water flux and power density. Power density, indicating how much benefit we can get from the system, has been extensively researched in the PRO system. However, the energy efficiency, evaluating the utilization degree of the Gibbs free energy of mixing from the draw and feed solutions, especially for closed loop systems or in the area with shortage of river water has been rarely investigated. A sensitivity analysis reveals that there exist different optimal hydraulic pressure differences leading to the maximum power density and energy efficiency, respectively. The performance of the PRO system under the maximum power density and energy efficiency is systematically investigated based on the GA method. The optimal hydraulic pressure difference corresponding to the maximum energy efficiency is larger than that corresponding to the maximum power density. Furthermore, an optimization based on NSGA-II was conducted to obtain the Pareto frontier which could indicate any compromise between the maximum power density and maximum energy efficiency. How to appropriately choose the final compromise solution in the Pareto frontier remains a dilemma, which should be determined by the local energy policies and technical and economic conditions of the PRO systems. For demonstration, the final compromise solution selected by the abstract heuristic TOPSIS method is discussed. And a desirable compromise between the power density and energy efficiency is presented.

Acknowledgments

We acknowledge the support received from the National Natural Science Foundation of China (51706076, 51736004). R. Long thanks the support from Laboratory of Mathematics for Nonlinear Science, Fudan University.

Nomenclature

J_w	Water flux m/s
J_s	Salt flux m/s
W	Membrane width mm
L	Channel length mm
H	Channel depth mm
V_D	Volume flow rate of draw solution L/min
V_F	Volume flow rate of feed solution L/min
$C_{D,b}$	Concentration of bulk draw solution g/L
$C_{F,b}$	Concentration of bulk feed solution g/L
$C_{D,m}$	Concentrations of the draw solution at the membrane side g/L
$C_{F,m}$	Concentrations of the feed solution at the membrane side g/L
$\Delta\pi_m$	Local osmotic pressure difference MPa
ΔP	Local hydraulic pressure difference across the membrane MPa
A	Water permeability coefficient m/(s•Pa)
B	Salt permeability coefficient m/s
K	Solute resistivity s/m
S	Support layer structural parameter m
D	Diffusion coefficient of the draw solution m^2/s
k	Local mass transfer coefficient in the draw solution m/s
P_{loss}	Local solution pressure loss MPa
ρ	Density kg/m^3
v	Cross flow velocity m/s
d_h	Hydraulic diameter m
λ	Friction coefficient
Re	Reynolds number
ΔP^0	Pressure difference of the draw and feed solutions at the inlet MPa
P_{PRO}	Power output W
$\bar{J}_w$	Average water flux m/s
P_d	Power density W/m^2
ΔG	Gibbs free energy W
R	Universal gas constant J/(mole•K)
C_T	Concentration of the mixed concentrated and diluted solutions g/L

Greek Symbols

η	Energy efficiency %

Subscripts

D	Draw solution
F	Feed solution
in	Inlet
out	Outlet
mix	mixing

Abbreviations

PRO	Pressure retarded osmosis
RED	Reverse electrodialysis
CAPMIX	Capacitive mixing
ICP	Internal polarization concentration
ECP	External polarization concentration
RSP	Reverse salt permeation
FO	Forward osmosis
DI	Deionized

References

[1] Long R, Li B, Liu Z, Liu W. Ecological analysis of a thermally regenerative electrochemical cycle. Energy 2016;107:95–102.
[2] Long R, Li B, Liu Z, Liu W. Hybrid membrane distillation-reverse electrodialysis electricity generation system to harvest low-grade thermal energy. J Membr Sci 2017;525:107–15.
[3] Long R, Li B, Liu Z, Liu W. Performance analysis of a thermally regenerative electrochemical cycle for harvesting waste heat. Energy 2015;87:463–9.
[4] Yip NY, Elimelech M. Thermodynamic and energy efficiency analysis of power generation from natural salinity gradients by pressure retarded osmosis. Environ Sci Technol 2012;46(9):5230.
[5] Achilli A, Childress AE, Cath TY. Power generation with pressure retarded osmosis: an experimental and theoretical investigation. J Membr Sci 2009;343(1–2):42–52.
[6] Weiner AM, Mcgovern RK, John HLV. A new reverse electrodialysis design strategy which significantly reduces the levelized cost of electricity. J Membr Sci 2015;493:605–14.
[7] Tufa Ramato A, Curcio E, Brauns E, van Baak W, Fontananova E, Di Profio G. Membrane distillation and reverse electrodialysis for near-zero liquid discharge and low energy seawater desalination. J Membr Sci 2015;496:325–33.
[8] Sales B, Saakes M, Post J, Buisman C, Biesheuvel P, Hamelers H. Direct power production from a water salinity difference in a membrane-modified supercapacitor flow cell. Environ Sci Technol 2010;44(14):5661–5.
[9] Altaee A, Zhou J, Alanezi AA, Zaragoza G. Pressure retarded osmosis process for power generation: feasibility, energy balance and controlling parameters. Appl Energy 2017;206:303.
[10] Long R, Kuang Z, Liu Z, Liu W. Temperature regulated reverse electrodialysis in charged nanopores. J Membr Sci 2018;561:1–9.
[11] Long R, Kuang Z, Liu Z, Liu W. Reverse electrodialysis in bilayer nanochannels: salinity gradient-driven power generation. Phys Chem Chem Phys 2018;20:7295–302.
[12] Sharqawy MH, Zubair SM, John HLV. Second law analysis of reverse osmosis desalination plants: an alternative design using pressure retarded osmosis. Energy 2011;36(11):6617–26.
[13] Helfer F, Lemckert C, Anissimov YG. Osmotic power with pressure retarded osmosis: theory, performance and trends – a review. J Membr Sci 2014;453:337–58.
[14] Yip NY, Elimelech M. Comparison of energy efficiency and power density in pressure retarded osmosis and reverse electrodialysis. Environ Sci Technol 2014;48(18):11002.
[15] Maisonneuve J, Laflamme CB, Pillay P. Experimental investigation of pressure retarded osmosis for renewable energy conversion: towards increased net power. Appl Energy 2016;164:425–35.
[16] He W, Wang Y, Shaheed MH. Maximum power point tracking (MPPT) of a scale-up pressure retarded osmosis (PRO) osmotic power plant. Appl Energy 2015;158:584–96.
[17] Qureshi BA, Zubair SM. Exergetic analysis of a brackish water reverse osmosis desalination unit with various energy recovery systems. Energy 2015;93:256–65.
[18] She Q, Jin X, Tang CY. Osmotic power production from salinity gradient resource by pressure retarded osmosis: effects of operating conditions and reverse solute diffusion. J Membr Sci 2012;401:262–73.
[19] Xu Y, Peng X, Tang CY, Fu QS, Nie S. Effect of draw solution concentration and operating conditions on forward osmosis and pressure retarded osmosis performance in a spiral wound module. J Membr Sci 2010;348(1):298–309.
[20] Fimbres-Weihs GA, Wiley DE. Review of 3D CFD modeling of flow and mass transfer in narrow spacer-filled channels in membrane modules. Chem Eng Process: Process Intensification 2010;49(7):759–81.
[21] Hancock NT, Cath TY. Solute coupled diffusion in osmotically driven membrane processes. Environ Sci Technol 2009;43(17):6769–75.
[22] He W, Wang Y, Shaheed MH. Modelling of osmotic energy from natural salt gradients due to pressure retarded osmosis: effects of detrimental factors and flow schemes. J Membr Sci 2014;471:247–57.
[23] Yip NY, Tiraferri A, Phillip WA, Schiffman JD, Hoover LA, Kim YC, et al. Thin-film composite pressure retarded osmosis membranes for sustainable power generation from salinity gradients. Environ Sci Technol 2011;45(10):4360–9.
[24] Kim YC, Lee JH, Park S-J. Novel crossflow membrane cell with asymmetric channels: design and pressure-retarded osmosis performance test. J Membr Sci 2015;476:76–86.
[25] Yaroshchuk A. Optimal hydrostatic counter-pressure in Pressure-Retarded Osmosis with composite/asymmetric membranes. J Membr Sci 2015;477:157–60.
[26] Kim YC, Elimelech M. Adverse impact of feed channel spacers on the performance of pressure retarded osmosis. Environ Sci Technol 2012;46(8):4673.
[27] Kim YC, Elimelech M. Potential of osmotic power generation by pressure retarded osmosis using seawater as feed solution: analysis and experiments. J Membr Sci 2013;429:330–7.
[28] Nagy E, Dudás J, Hegedüs I. Improvement of the energy generation by pressure retarded osmosis. Energy 2016;116:1323–33.
[29] He W, Wang Y, Shaheed MH. Energy and thermodynamic analysis of power generation using a natural salinity gradient based pressure retarded osmosis process. Desalination 2014;350:86–94.
[30] Han G, Ge Q, Chung T-S. Conceptual demonstration of novel closed-loop pressure retarded osmosis process for sustainable osmotic energy generation. Appl Energy 2014;132:383–93.
[31] Anastasio DD, Arena JT, Cole EA, McCutcheon JR. Impact of temperature on power density in closed-loop pressure retarded osmosis for grid storage. J Membr Sci 2015;479:240–5.
[32] Long R, Lai X, Liu Z, Liu W. A continuous concentration gradient flow electrical energy storage system based on reverse osmosis and pressure retarded osmosis. Energy 2018;152:896–905.
[33] Loeb S, Mehta GD. A two-coefficient water transport equation for pressure-retarded osmosis. J Membr Sci 1978;4(00):351–62.
[34] Prante JL, Ruskowitz JA, Childress AE, Achilli A. RO-PRO desalination: an integrated low-energy approach to seawater desalination. Appl Energy 2014;120:104–14.
[35] Lee KL, Baker RW, Lonsdale HK. Membranes for power generation by pressure-retarded osmosis. J Membr Sci 1981;8(2):141–71.
[36] Tiraferri A, Yip NY, Straub AP, Romero-Vargas Castrillon S, Elimelech M. A method for the simultaneous determination of transport and structural parameters of forward osmosis membranes. J Membr Sci 2013;444:523–38.
[37] Achilli A, Cath TY, Childress AE. Power generation with pressure retarded osmosis: an experimental and theoretical investigation. J Membr Sci 2009;343(1):42–52.
[38] Schwinge J, Neal PR, Wiley DE, Fletcher DF, Fane AG. Spiral wound modules and spacers : review and analysis. J Membr Sci 2004;242(1–2):129–53.
[39] Sadeghian RB, Pantchenko O, Tate D, Shakouri A. Miniaturized concentration cells for small-scale energy harvesting based on reverse electrodialysis. Appl Phys Lett 2011;99(17):173702–3.
[40] Long R, Li B, Liu Z, Liu W. Performance analysis of a dual loop thermally regenerative electrochemical cycle for waste heat recovery. Energy 2016;107:388–95.
[41] Long R, Li B, Liu Z, Liu W. Performance analysis of reverse electrodialysis stacks: channel geometry and flow rate optimization. Energy 2018;158:427–36.
[42] Long R, Li B, Liu Z, Liu W. Multi-objective optimization of a continuous thermally regenerative electrochemical cycle for waste heat recovery. Energy 2015;93(Part 1):1022–9.
[43] Long R, Li B, Liu Z, Liu W. Reverse electrodialysis: modelling and performance analysis based on multi-objective optimization. Energy 2018;151:1–10.
[44] Long R, Lai X, Liu Z, Liu W. Direct contact membrane distillation system for waste heat recovery: modelling and multi-objective optimization. Energy 2018;148:1060–8.